

Glutaraldehyde-crosslinking for improved copper absorption selectivity and chemical stability of polyethyleneimine coatings

Johan B. Lindén^a, Mikael Larsson^{a, b}, Simarpreet Kaur^a, Ataollah Nosrati^c and Magnus Nydén^{a, b}

^aFuture Industries Institute, University of South Australia, Mawson Lakes, SA, 5095, Australia.

^bSchool of energy and resources, University College London, 220 Victoria Square, Adelaide, SA, 5000, Australia.

^cSchool of Engineering, Edith Cowan University, 270 Joondalup Drive, Joondalup WA, 6027, Australia.

Correspondence to: M. Larsson (E-mail: larsson.mikael@gmail.com)

ABSTRACT

Nano-thin coatings of glutaraldehyde (GA)-crosslinked polyethyleneimine (PEI) are extremely selective and effective in binding copper from seawater. Here it was demonstrated that GA-PEI performs significantly different from PEI. The selectivity towards copper of self-assembled PEI coatings on silicon substrates was greatly improved by GA-crosslinking. After submersion of coatings in artificial seawater containing 200 ppb copper and equimolar amounts of 11 competing ions only copper and trace amounts of Zn were detected in the GA-crosslinked coatings, while for non-crosslinked PEI there was about 30% Zn present relative to copper. The coatings were demonstrated to be highly stable under acidic conditions and retained the copper-binding selectivity after repeated cycles of binding and acid-mediated elution. After self-assembly of the material on mesoporous diatomaceous earth particles, to create 3-D samples rather than the 2-D surfaces, copper could be extracted from 200 ppb in artificial seawater and eluted under acidic pH.

Keywords: Acid stability; Artificial seawater; Copper selectivity; Glutaraldehyde; Polyethyleneimine; Self-assembled coatings

INTRODUCTION

In the human body metals facilitate many essential functions, e.g. transport of oxygen and redox reactions.¹ There are disease conditions associated with excess metal accumulation that are treated with metal chelating drugs² and there is indication that copper-chelating materials have potential for novel treatments of cancer and cardio vascular diseases.^{3,4} Further, metal binding is essential in for example catalysis,⁵ metal ion sensing,^{6,7} recovery of waste materials in aqueous solutions,⁸ mining processes,⁹ heavy metal removal from waste waters^{10,11} and removal of metal pollutants from natural waters like rivers and seawater.¹²

Polyethyleneimine (PEI) effectively binds copper¹³⁻¹⁹ and other metals²⁰⁻²² in basic and mildly acidic conditions. However, the binding efficacy and specificity varies between reports.^{23,24} Even though PEI is commonly crosslinked with glutaraldehyde (GA) to create a stable coating,^{19,20,25,26} there seem to be little knowledge on how the crosslinking impacts the specificity in binding of different metals. Based on previous observations that nano-thin coatings of GA-crosslinked PEI coatings were remarkably selective towards copper in artificial²⁷ and real seawater,²⁸ we here study the effect of GA-crosslinking on copper uptake in more detail. From an application point of view it is important that the copper can be released and that the absorption material can be reused many times.²⁶ One simple way to release the copper is to immerse the absorption material in acidic solution, pH below 2. We therefore studied the stability of GA-crosslinked PEI coatings under varying acidic conditions. Finally, with the current issue of copper-contaminated harbors^{29,30} in mind, the uptake and release efficiency of the material was evaluated in artificial seawater. To this end the nano-thin coating material was self-assembled onto mesoporous silica carriers in the form of diatomaceous earth particles to have a large surface area available for copper absorption. Such silica-polyamine composite material could also be of interest for other applications, e.g. catalysis.³¹

Coatings for copper uptake and selectivity studies were prepared by self-assembly of PEI onto silicon substrates, with and without subsequent crosslinking with GA. The self-assembly and stability of the coatings in artificial seawater and under acidic conditions was investigated using quartz crystal microbalance with dissipation monitoring (QCM-D). The metal ion uptake from artificial seawater was characterized by X-ray photoelectron spectroscopy (XPS). The surface topography of the samples was investigated using atomic force microscopy (AFM). Finally, to evaluate the feasibility of re-utilizing GA-crosslinked PEI for remediation of copper-contaminated harbors, the coating material was exposed to cycles of copper-uptake in artificial seawater and release under acidic conditions. Finally, inductively coupled plasma mass spectrometry (ICP-MS) was used to evaluate the potential for remediation of copper-contaminated harbors by studying extraction efficiency from artificial seawater.

EXPERIMENTAL

Materials

All chemicals were of analytical or reagent grade and were used as received without further purification. Sea Salt (40 g/L) (Sigma Aldrich, Australia) was used to prepare artificial seawater. Branched polyethyleneimine (PEI) (50 wt% in H₂O, Mn ~ 60,000 g/mol and MW ~ 750,000 g/mol) (Sigma Aldrich, Australia), glutaraldehyde (GA) (grade II, 25 wt% in H₂O) (Sigma Aldrich, Australia) and

sodium chloride (Chem-Supply, Australia) were used for preparation of GA-crosslinked PEI coatings and were stored under N₂. Solutions of hydrochloric acid (36 %) (Ajax Finechem, Australia) and sodium hydroxide (Chem-Supply, Australia) were used to adjust the pH of solutions. Aluminum(III) chloride hexahydrate, cadmium(II) nitrate tetrahydrate, cobalt(II) chloride hexahydrate, chromium(III) nitrate nonahydrate, iron(II) sulphate heptahydrate, manganese(II) sulphate monohydrate, nickel(II) nitrate hexahydrate, sodium molybdate(VI) dehydrate and vanadium(III) chloride were all purchased from Sigma Aldrich (Australia) and used to spike artificial seawater. Lead(II) nitrate (May & Baker, Australia), zinc(II) chloride (Scharlau, Australia) and copper(II) sulphate pentahydrate (Chem-Supply, Australia) were also used to spike artificial seawater. Dilutions of nitric acid (70 wt%) (Chem-Supply, Australia) was used for acid stability tests and nitric acid (≥ 69%, TraceSELECT[®], for trace analysis) (Sigma Aldrich, Australia) was used for copper elution and preparation of solutions for ICP-MS analysis. Silicon wafers (4", CZ, <100>, Boron (P), 0.5-100 ohm.cm, 400 μm, SSP) were acquired from Electronics and Materials Ltd. Ultrapure water (MQ-water) with a resistivity of 18.2 MΩ cm was obtained using a Milli-Q[®] Advantage A10[®] water purification system and was used for preparation of all dispersions and solutions.

pH measurements

The pH measurements were conducted using an ION 700 meter equipped with a pH electrode (Eutech instruments, Singapore). Prior to measurements a three-point calibration was performed using pH 4, 7 and 10 calibration buffers (Sitest Pty. Ltd., Australia).

Quartz crystal microbalance with dissipation monitoring (QCM-D)

The self-assembly of PEI from solutions with different concentrations (0.05, 0.1 and 0.2 wt% PEI), crosslinking and acid stability of crosslinked and non-crosslinked PEI coatings on silicon dioxide was monitored by quartz crystal microbalance with dissipation (QCM-D) (E4, Q-sense, Sweden) using silica coated AT-cut 5 MHz quartz crystals purchased from Q-sense, Sweden. Prior to measurements the sensors were cleaned by treatment for 10 minutes in a UV-ozone cleaner (Bioforce Nanosciences, USA), followed by sonication for 30 minutes in 2% SDS solution, submersion in excess MQ-water, extensive rinsing with MQ-water, drying with N₂ gas and finally another 15 minutes of UV-ozone treatment. All experiments were performed in quadruplicates and run simultaneously with a flow rate of 0.1 mL/min. Multiple overtones (3rd, 5th, 7th, 9th, 11th and 13th) were recorded. The 5th overtone was selected and analyzed for all sensors. The mass of the adsorbed PEI was estimated using the Sauerbrey relationship (1), where C = 17.7 ng Hz⁻¹ cm⁻² for a 5 MHz quartz crystal, n is the overtone number and Δf is the frequency change induced by PEI adsorption.

$$\Delta m = -\frac{C\Delta f}{n} \quad (1)$$

To validate the Sauerbrey relationship the adsorbed layer needs to be deemed sufficiently rigid which is generally considered when the ratio of ΔD/(-Δf/n) is less than 4 x 10⁻⁷.^{32,33}

Zeta potential of PEI as a function of pH

The zeta potential of polyethyleneimine (PEI) in solution (2 mg/mL in 1 mM KCl) was determined using disposable folded capillary cells (DST1070) and a Nano-ZS Zetasizer (Malvern Instruments Ltd., Worcestershire, UK) in electrophoretic light scattering mode. Separate solutions were prepared for each pH and prepared with 1 M HCl and 0.02 M KOH. The temperature was set to 23 °C and the sample was equilibrated in the instrument for 120 seconds before start of measurement. Attenuation and voltage were automatically adjusted to obtain the optimum data quality and the Smoluchowski model was then used to calculate the zeta potential values from the dynamic mobility data.

X-ray photoelectron spectroscopy (XPS)

X-ray photoelectron spectroscopy (XPS) analysis was conducted on a Kratos Axis-Ultra spectrometer using monochromatized Al K α X-rays (1486.7 eV) at a power of 225 W (160 eV analyzer pass energy for survey scans, 20 eV for high-resolution scans). The spot size for analysis was $\sim 300 \times 700 \mu\text{m}$. Core electron binding energies are given relative to an adventitious hydrocarbon C 1s binding energy of 284.8 eV. The elemental composition within a sample was determined as an average of analysis of two spots per sample. The coordination of the metals to nitrogen in the coating was evaluated by the atomic ratios of metal to nitrogen.

Atomic force microscopy (AFM)

The surface topography of crosslinked and non-crosslinked coatings on silicon wafers was investigated using atomic force microscopy (AFM). ScanAsyst was used in air on a Nanoscope MultiMode 8 AFM (Bruker) with a Nanoscope V controller. WSxM v5.0 Develop 8.0 software from WSxM solutions (www.wsxmsolutions.com) was used to process the data.³⁴

Solution-based inductively coupled plasma - mass spectrometry (ICP-MS)

Trace element concentrations were measured with a solution-based inductively coupled plasma mass-spectrometry (ICP-MS) (Agilent 7500ce, Agilent Technologies, Tokyo, Japan), equipped with an octopole collision system for the removal of polyatomic interferences. The ICP-MS was equipped with a Miramist nebulizer and a quartz spray chamber. An internal standard (Indium) was mixed online with the samples to compensate for matrix effects. All element concentrations were determined against certified multi-element calibration standards (Choice Analytical, Australia) and blanks were interspersed throughout the analysis session, and several measurements using the calibration solutions were performed to ensure instrument stability. The instrument was operated with an RF power of 1500 W, a carrier gas flow of 0.89 L/min and a make-up gas flow of 0.19 L/min. Sample uptake rate was 1.0 mL/min and the dwell times ranged between 10ms to 50ms. Three replicates were obtained for each sample. The data was processed using Agilent MassHunter Data Analysis™.

Preparation of solutions for QCM-D

Solutions of PEI (MW 750,000) for self-assembly on silica-coated QCM-D crystals were prepared in three different concentrations (0.05, 0.1 and 0.2 wt%) in 0.5 M NaCl and adjusted to pH 9 with HCl (1 M). As control, a solution of 0.5 M NaCl pH 9 was prepared to monitor the influence of the solvent density and viscosity on frequency and dissipation. Solutions of hydrochloric acid (1 M) and nitric acid (1 M) were used for the acid stability tests. GA (0.5 wt% in H₂O) was used for crosslinking. Artificial seawater (pH ~ 8.1) was prepared by dissolving sea salt (40 g/L) in MQ-water.

Self-assembly of PEI on silicon wafers

Silicon wafers were manually cut into ~ 1 cm² squares. The pieces were washed by sonication in 2% RBS 35 detergent solution (Thermo Scientific, USA) for 15 minutes, rinsing with MQ-water, sonication in MQ-water for 5 minutes, rinsing with MQ-water and submersion in ethanol for storage. Prior to use the pieces were rinsed with ethanol and dried with N₂ gas. PEI self-adsorption was achieved by immersion of each sample in 5 mL solution of PEI (0.2 wt%, 0.5 M NaCl, pH 9) for 30 minutes. Thereafter, any loosely bond PEI were removed by immersion of the samples in solutions of 5 mL MQ-water (repeated three times).

Crosslinking of self-assembled PEI on silicon wafers

Following the removal of loosely attached PEI of the self-assembly procedure, each sample was immersed in 5 mL of GA solution (0.5 wt% in H₂O) for 30 minutes. Thereafter, any unreacted GA was removed by immersing the samples in three solutions of 5 mL MQ-water after which the samples were gently dried with N₂.

Metal ion uptake by crosslinked and non-crosslinked PEI in artificial seawater

The selectivity of crosslinked and non-crosslinked PEI was evaluated in artificial seawater with twelve added seawater-relevant metal ions: aluminum, cadmium, cobalt, chromium, copper, iron, manganese, molybdenum, nickel, lead, vanadium and zinc. The artificial seawater was prepared by dissolving sea salt (40 g/L) in MQ-water (pH ~ 8.1). Stock solutions of the metal ions (100 mM: Al, Cd, Co, Cr, Cu, Mn, Mo, Ni, Pb, V and 2 mM: Fe, Zn) were prepared in MQ-water and added to the artificial seawater to achieve equimolar concentration of ~ 3.15 μM. This corresponds to 85 ppb Al, 354 ppb Cd, 185 ppb Co, 164 ppb Cr, 200 ppb Cu, 176 ppb Fe, 173 ppb Mn, 302 ppb Mo, 185 ppb Ni, 652 ppb Pb, 160 ppb V and 206 ppb Zn. Samples of self-assembled PEI on silicon wafer pieces (~ 1 cm², squares) were immersed individually in glass bottles containing 23 mL of metal-spiked artificial seawater. Triplicate samples were taken up at selected times, washed by immersion in three solutions of 5 mL MQ-water and dried with N₂ before further characterization.

Statistical analyses

All statistical analyses were performed using OriginPro 8 (OriginLab Corporation) statistical software program. Statistical significant differences between means were determined using two-sample t-tests.

Cycling of selective uptake and release

Cycling of selective metal ion uptake and release in artificial seawater was performed with samples of self-assembled and crosslinked PEI on silicon wafer pieces ($\sim 1 \text{ cm}^2$, squares). Samples were immersed for 2 hours in artificial seawater (23 mL/sample) containing 12 seawater relevant metals (Al, Cd, Co, Cr, Cu, Fe, Mn, Mo, Ni, Pb, V and Zn. $[\text{Me}] \sim 3.15 \mu\text{M}$) for uptake and thereafter immersed for 2 hours in MQ-water with pH adjusted to ~ 1 using hydrochloric acid (1 M) for release.

Preparation of PEI modified mesoporous diatomaceous earth (DE) particles

Fine DE powder (Diatomaceous Earth Online TM; Queensland, Australia) was purified via acid treatment at $100 \text{ }^\circ\text{C}$ using 1 M H_2SO_4 for 2h, followed by replenishing of the solution and treatment at $100 \text{ }^\circ\text{C}$ using 3 M H_2SO_4 for 20h, all under magnetic stirring. Modification with GA-crosslinked PEI was then performed as follows: The particles were dispersed to 10 wt% in 40 ml of 1 wt% PEI in 0.5 M aqueous NaCl solution in 50 ml Falcon tubes. The dispersion was ultrasonicated (Soniclean, Australia) for 15 minutes followed by mixing for 30 minutes on a rotary mixer and then centrifuged at 4700 rpm (RCF = 4643) for 5 minutes using a Sigma 416K centrifuge and the supernatant was discarded. The pellet was washed by re-dispersion in 100 ml MQ-water for 5 minutes and repetition of the centrifugation step. After repeating the washing three times the pellet was re-dispersed in 40 ml of 0.5% GA in water, followed by incubation for 30 minutes on the rotary tube mixer before centrifugation and discarding of supernatant. Finally, the product was washed twice with 100 ml of MQ-water, as described above. All reactions and processes were conducted at room temperature.

Prior to use the modified particles were further purified according to the following protocol to prevent PEI leaching from the particles. 2.5 g of DE particles were dispersed in 100 mL of MQ-water, followed by agitation at room temperature for 60 minutes. The dispersion was centrifuged at 4700 rpm for 3 minutes and the supernatant was discarded. The DE particles were re-dispersed in 100 mL of MQ-water and the pH was adjusted to ~ 1 using small amounts of 1 M hydrochloric acid. After agitation for 10 minutes the dispersion was centrifuged as above, the supernatant discarded, the DE particles re-dispersed in 100 mL MQ-water and the pH was adjusted to ~ 10 using small amounts of 1 M sodium hydroxide. The dispersion was agitated for 10 minutes before centrifuged as above, the supernatant was discarded and the DE particles were re-dispersed in 100 mL artificial seawater, with pH ~ 9 . It was further agitated for 10 minutes and centrifuged as above, supernatant was discarded and the DE particles re-dispersed in 100 mL artificial seawater, followed by adjustment of the pH to ~ 8.1 with small amounts of 1 M hydrochloric acid. Subsequently, the dispersion was agitated overnight before centrifuged as above. The supernatant was discarded and the DE particles collected.

Extraction of copper in artificial seawater

2.5 g of PEI-modified DE particles were dispersed in 100 mL of artificial seawater with 100 ppb of added copper in the form of CuSO_4 , followed by agitation for 24 hours. Dispersion was centrifuged at 4700 rpm for 3 minutes and the copper loaded particles were centrifuged down as above and re-dispersed two times in 100 mL MQ-water to remove non-bound copper and highly saline water, which otherwise would interfere with the ICP-MS characterization. Copper-loaded DE particles were re-dispersed in 100 mL MQ-water and 1.1 mL of nitric acid (high purity) was added to lower the pH to ~ 1 for desorbing the copper from the coating. The particles were separated from the elution solution by centrifugation, as above, and the copper concentration in the solution was determined by ICP-MS.

RESULTS AND DISCUSSION

Self-assembly of PEI on silica coated QCM-D sensors

PEI self-assembly from 0.05, 0.1 and 0.2 wt% PEI solutions in 0.5 M NaCl and pH 9 onto silica was monitored using QCM-D by recording changes in frequency and dissipation. The frequency and dissipation depend on the properties of the bulk fluid, such as density and viscosity, but more importantly they respond to changes in mass and viscoelastic properties of material adsorbing on the surface of the sensor. In Figure 1 the top and bottom panels display the frequency and dissipation responses, respectively. In the first 45 minutes of the experiment the baseline behavior was determined for MQ-water (MQ) and artificial seawater (AS). It was noted that when changing from MQ to AS the frequency decreased and the dissipation increased, likely caused by differences in densities and viscosities between the solvents. The sensors were then stabilized in 0.5 M NaCl pH 9 (NaCl), the same condition used in subsequent PEI-adsorption steps. The relatively high pH and ionic strength facilitated the formation of a thick and compact layer of self-assembled PEI.³⁵⁻³⁷ The pH was chosen based on a previously reported protocol for self-assembly of PEI³⁷ and zeta potential measurements that showed how increasing the pH above 9 significantly decreased the polymer charge (Figure 2). The reason for wanting as high pH as possible without reducing the positive charge of PEI is that the silica becomes increasingly negatively charged with increasing pH, which promotes the electrostatic interaction. The self-assembly behavior as function of PEI concentration was investigated by exposing the sensors to three adsorption steps: 0.05 wt% (PEI 1); 0.1 wt% (PEI 2) and; 0.2 wt% (PEI 3). Between each step sensors were rinsed with the following solutions (in order): MQ; AS; 0.5 M NaCl pH 9 (NaCl); 1 M HCl (HCl); MQ; AS; and; 0.5 M NaCl pH 9 (NaCl) for correct establishment of the frequency and dissipation change in each solvent and for cleaning the sensors from PEI before a new adsorption step.

The adsorption behavior of PEI was similar for all three PEI solutions; a rapid initial adsorption was followed by a slower process. Such adsorption behaviour was interpreted by Mészáros et al. as follows; in the initial adsorption stage the rate-determining step is the diffusive transport of PEI from the bulk.³⁵ As the surface coverage increases an electrostatic barrier is formed that slows down the adsorption, which eventually becomes the rate-limiting step. The electrostatic barrier was explained as the sum of the attractive forces between polymer segments and the surface and the repulsive forces between polymer segments. When re-applying MQ, AS and NaCl after PEI adsorption, the frequency stabilised at lower values and the dissipation stabilised at higher values, compared to clean sensor in the corresponding solvent. The changes in frequency and dissipation were attributed to the adsorbed PEI layer and were in qualitative agreement between all solvents. Importantly, after rinsing

with HCl the frequency and dissipation values reverted to those of clean sensors in each solvent, which proved that acid rinsing removed the PEI. As seen in Table 1 all three PEI concentrations resulted in a 15 - 17 Hz decrease in frequency and about 2×10^{-6} increase in dissipation, suggesting that for all concentrations a rigid PEI layer ($\Delta D/(-\Delta f/n) < 4 \times 10^{-7}$)^{32,33} was formed with a thickness of 2.5 - 3 nm, as estimated by the Sauerbrey relationship.³⁸ The fact that no difference was detected between the layers formed from the different PEI concentrations indicated that the surface became saturated with PEI already at the lowest PEI concentrations and that the bulk changes at higher PEI concentrations did not alter the surface behaviour of PEI.

Crosslinking and acid stability of crosslinked and non-crosslinked coatings

GA is a dialdehyde extensively used in the crosslinking of materials containing primary amines. The GA-crosslinking of self-assembled PEI was monitored by QCM-D (Figure 3). Here the PEI was first self-assembled using 0.2 wt% (0.5 M NaCl in MQ-water pH 9) and rinsed with MQ. After stabilizing in MQ, the sensors were exposed to GA (0.5 % in MQ). The crosslinking reaction seems to take place within the first 15 minutes with a corresponding frequency shift of -10 Hz (corresponding to a mass gain of about 180 ng/cm^2).³⁸ The decrease in frequency corresponded to a mass increase of about 60%, proving that the coatings were highly crosslinked. A slight decrease in dissipation was noted after crosslinking, indicating a small increase in rigidity. This should not be seen as an indication of the highly crosslinked coating being soft, rather that the excessive crosslinking only slightly affected the dissipation since the self-assembled PEI layer on silica was already quite rigid, as discussed in section 3.1.

AFM was performed to study the impact of crosslinking on surface topography. From Figure 4 it is apparent that the topography of the material was different after crosslinking. Roughness analysis of the surface scans revealed a root mean square (RMS) roughness value of 1.25 nm for the crosslinked PEI in comparison to and 0.69 nm for non-crosslinked PEI (Table 2). This is also shown in the relative height histograms where the average height changed from 2.9 to 3.6 nm and a skewness was present after crosslinking. For further details on replicates and roughness analysis see Figures S1 – S5 and Table 2.

The acidic stability of the GA-crosslinked PEI coatings was evaluated in 1 M of HCl and HNO₃. As a control experiment identical stability tests were conducted for non-crosslinked PEI coatings. As expected, for non-crosslinked coatings the PEI was completely removed by both acids (Figure 5A). Under acidic conditions silica surfaces becomes less negatively charged and PEI becomes highly protonated.³⁶ Thus, upon acidifying the solution the attraction forces between the PEI and the silica surface decreased and electrostatic repulsive forces and high osmotic pressure from the PEI counterions caused dissociation of the coating.

In contrast to the non-crosslinked PEI, coatings of GA-crosslinked PEI were stable upon exposure to both acids, as seen from the QCM-D sensogram in Figure 5B. After crosslinking the frequency and dissipation were similar before and after exposure to acid for a given solvent.

At first glance the acid stability of the crosslinked coatings may seem surprising as GA reacts with amines to form Schiff's bases, which are known to be reversible under acidic conditions. However, it

has been reported that GA-crosslinking of amines presents exceptional stability at extreme temperatures and pH.³⁹ This stability was explained by aldol condensation polymerization of GA proceeding in parallel with the crosslinking reaction, with a dehydration reaction producing ethylenic double bonds conjugated with the imine bonds. Based on the QCM-D results it was concluded that the GA-crosslinking of the PEI coatings produced a material with excellent acid stability. With the application of interest in mind, both crosslinked and non-crosslinked PEI coatings were also shown to be stable in artificial seawater (Figure S6).

Metal ion selectivity

Nano-thin spin coated PEI coatings crosslinked with GA have previously been shown to effectively absorb copper from seawater relevant concentrations (2 – 200 ppb) in artificial seawater²⁷ and natural seawater.²⁸ Furthermore, the coatings were proven to be highly selective to copper in artificial seawater containing 12 seawater-relevant metals. Interestingly, a time-dependent binding process was revealed with zinc being present in the coatings at early times, but being replaced by copper over time. This phenomenon was shown to be inherent to copper and zinc and did not depend on the other metals. The behavior was also observed in natural seawater.

Further investigation by FTIR and synchrotron XANES indicated that the structure of the PEI changed into a network with high content of imine groups (Schiff's bases) upon crosslinking with GA.²⁸ The change in chemical environment likely affected the affinity and selectivity towards copper. In an attempt to elucidate the effects of GA-crosslinking of PEI on the selectivity towards copper in seawater, samples of GA-crosslinked and non-crosslinked PEI were immersed in artificial seawater with 12 seawater relevant metal ions at equimolar concentrations. The metal uptake in the nano-thin coatings was evaluated over time from the ratio of metal to nitrogen (Me/N), as determined by XPS. The binding of copper was independent on the crosslinking, while the binding of zinc was decreased dramatically with crosslinking (Figure 6 A and B). Non-crosslinked coatings had absorbed large amounts of zinc already after 1 minute. Over time the zinc content decreased and plateaued at a Zn/N ratio of about 0.05 after 16 minutes. In contrast, the absorption of zinc into the crosslinked coatings was slower, with a maximum Zn/N ratio of about 0.05 at 4 minutes, after which the concentration decreased towards zero. The results indicated that the extreme copper selectivity of the material could be attributed to the crosslinking with GA. It is also worth noting that no other metal ions were detected in the coatings independent of the material being crosslinked or not, which was surprising considering other reports on the affinity of PEI to some of the tested metals.²⁰⁻²²

The error-bars in Figure 6 A and B represent the standard deviation and illustrate the spread of the data. Although the trends were quite clear in the results, further experiments were conducted to ensure statistically significant differences. Nine replicates were performed at the 128 minutes time-point where the plateau was considered to have been reached. Figure 7 shows the average copper and zinc content (expressed as metal-to-nitrogen ratio) in crosslinked and non-crosslinked PEI coatings after immersion in artificial seawater for 128 minutes, with error-bars representing the standard error of the mean. With the larger number of replicates a small decrease in copper content was observed for the GA-crosslinked coating compared to the PEI. However, more importantly, the zinc content was still dramatically decreased in the GA-crosslinked coatings compared to in the PEI. Differences between the means of the crosslinked and non-crosslinked PEI coatings were tested with two-sample

one-sided t-tests, with the null hypothesis that there was no difference between the coatings. From the t-tests it was concluded that the GA-crosslinked PEI absorbed less copper ($p < 0.02$) and zinc ($p < 0.001$) than the non-crosslinked PEI. Although a significant difference was observed for copper and zinc, the reduction in metal content was much more pronounced for zinc. In conclusion, the GA-crosslinking of PEI coatings resulted in a slight decrease in the amount of absorbed copper at the investigated conditions, but the selectivity towards copper was much improved.

The applicability for copper remediation and/or copper concentration purposes is strongly dependent on the capacity to regenerate and reuse the coating material with sustained performance.¹⁹ A porous silica gel with surface bound PEI has previously been shown to have regenerative capacity in waste water applications after several cycles of uptake and release by acid elution.¹⁴ The copper chelating property of GA crosslinked PEI on a cation-exchange resin has also been shown to withstand regeneration using different acids.¹⁹ However, to the best of our knowledge, there are no studies showing how the selectivity of GA-crosslinked PEI coatings towards copper in presence of other metal ions is affected by such regeneration. In section 3.2 it was shown how GA-crosslinking of self-assembled PEI on silica increased the stability upon exposure to acidic conditions. To test the potential of the material reported here for release of the absorbed metal ions by acid elution and for sustained copper uptake capacity and selectivity after regeneration, it was exposed to 10 cycles of uptake and release. The silicon wafers with nano-thin GA-crosslinked PEI were immersed for 2 hours in artificial seawater for uptake and then immersed for 2 hours in MQ-water at $\text{pH} \sim 1$ for release. As seen in Figure 8, the copper uptake capacity remained at roughly the same level throughout the 10 cycles and the selectivity for copper was maintained. Very low levels of zinc were observed in the coatings after 1st and 5th uptake cycle and no zinc was observed after the 10th cycle. Again no other metal ions were detected in the coatings.

Analysis by AFM showed very little change in the surface topographies after the 10th cycle of uptake and release compared with the crosslinked coating before any exposure (Figure 9). Replicates and roughness analysis details are presented in Figures S1 – S5 and Table 2. The results showed that the crosslinked coating could be reused without changes to the surface topography. Taken together the AFM analyses, QCM-D data and maintained metal binding performance proved the coatings to be stable and maintain performance over repeated uptake-elution cycles.

Extracting copper from artificial seawater

Having established that GA-crosslinking of PEI increased the copper selectivity and that the affinity and selectivity for copper was retained over several cycles of uptake and release, the potential for remediation of copper-contaminated seawater was investigated in simple a model system. Briefly, PEI was self-assembled (adsorbed) onto DE particles, followed by GA-crosslinking. A large excess of the modified DE-particles was then added to artificial seawater spiked with 200 ppb copper in the form of CuSO_4 . After agitation overnight the particles were separated from the solution by centrifugation. Subsequently, the particles were washed and the copper was eluted in MQ-water at $\text{pH} \sim 1$ to the same volume as for the copper uptake process. The concentration measured in the elution solution was determined by ICP-MS to 199 ppb (± 2 ppb, $n = 3$). It was thus concluded that the crosslinked PEI on DE particles was highly effective in absorbing copper from artificial seawater at levels relevant to contaminated harbors⁴⁰⁻⁴² and that the material holds potential for remediation applications.

However, in natural seawater the majority of copper (>99 %) is bound to organic ligands with high stability constants which would compete with the copper extracting material.⁴³ The sources and structures of those ligands are however under current investigation⁴⁴ and likely vary depending on season and location. Thus, more elaborative studies using model systems as well as real seawater samples from several locations during different seasons will be required to determine and understand the performance of the material under different conditions.

From an applications point, the process as described here would need to be further engineered to enable extraction of copper from the sea at large scale. Given the low concentration of copper in the sea (1-10 ppb) and the large volumes that would need to be processed, it would be too costly to pump water through the adsorption material. We envisage therefore that a more suitable design uses the motion of waves, currents and tidal movements, with as little external energy as possible, to continuously expose the material to fresh seawater from which copper is bound. The design would also need to take into account release of copper for re-use of the material and potentially concentration of the copper into a solution that for instance can be used in the electrowinning process of making metallic copper. This work is also under progress in our group.

CONCLUSIONS

Nano-thin PEI coatings were formed on macroscopic silica surfaces and on diatomaceous earth particles. The thickness of the coating was independent on the concentration of PEI in solution. A rapid crosslinking reaction took place when exposing the coatings to glutaraldehyde, making the coatings mechanically and chemically stable under acidic conditions. While the crosslinking increased the roughness of the coating surface it maintained high absorption capacity for copper and, importantly, significantly increased the coating's selectivity towards copper. The highly efficient and selective copper uptake and the topography of the coating surface were shown to be sustained after 10 cycles of competitive uptake in artificial seawater and release by elution under acidic conditions. Highly efficient removal of copper from artificial seawater was shown feasible with the GA-crosslinked PEI coating on diatomaceous earths particles as carrier material, indicating potential for extraction of copper from contaminated seawater. However, due to the complex environment in natural seawater further studies are needed under more challenging conditions, both in model and real systems, to establish the impact of various environmental factors on the performance. Finally, we note with applications in mind, that the preparation process of the glutaraldehyde-crosslinked PEI coatings is based on self-assembly and reaction by simple mixing at room temperature in water. Although the preparation method used in this paper for academic purposes involved several centrifugation steps the process can be easily upscaled to larger volumes where separation between steps is by filtration or even sedimentation. Furthermore, the process is transferrable to other silica-based porous substrates. Upscaling and investigation of other substrates is a subject of our future work and promising results have been achieved in early experiments.

ACKNOWLEDGEMENTS

The project is supported by the Premier's Research and Industry Fund grant provided by the South Australian Government Department of State Development. The authors would like to thank Ms. Aoife McFadden from Adelaide Microscopy (The University of Adelaide) for help with solution ICP-MS analysis and Dr. Magnus Röding for his advice on statistical analysis.

SUPPORTING INFORMATION

Zeta potential of PEI as a function of pH; QCM-D sensogram of the cross-linking of self-assembled PEI on silica-coated QCM sensors; QCM-D sensogram of the stability of non-crosslinked and crosslinked self-assembled of PEI on silica-coated QCM sensors in artificial seawater; AFM height images and roughness analysis of PEI coatings on silicon wafer after self-assembly, crosslinking and cycles of copper uptake and release.

REFERENCES

1. Crichton, R. R. In *Biological Inorganic Chemistry*; Crichton, R. R., Ed.; Elsevier: Amsterdam, **2008**; pp 1-12.
2. Franz, K. J. *Dalton Trans.* **2012**, 41, 6333.
3. Brewer, G. J. *Drug Discovery Today* **2005**, 10, 1103.
4. Mandinov, L.; Mandinova, A.; Kyurkchiev, S.; Kyurkchiev, D.; Kehayov, I.; Kolev, V.; Soldi, R.; Bagala, C.; de Muinck, E. D.; Lindner, V.; Post, M. J.; Simons, M.; Bellum, S.; Prudovsky, I.; Maciag, T. *Proc. Natl. Acad. Sci. U. S. A.* **2003**, 100, 6700.
5. Cozzi, P. G. *Chem. Soc. Rev.* **2004**, 33, 410.
6. Wen, T.; Qu, F.; Li, N. B.; Luo, H. Q. *Arabian Journal of Chemistry* **2013**, DOI: 10.1016/j.arabjc.2013.06.013.
7. Yuan, Z.; Cai, N.; Du, Y.; He, Y.; Yeung, E. S. *Anal. Chem.* **2013**, 86, 419.
8. Chassary, P.; Vincent, T.; Sanchez Marciano, J.; Macaskie, L. E.; Guibal, E. *Hydrometallurgy* **2005**, 76, 131.
9. Torres, R.; Blesa, M. A.; Matijević, E. *J. Colloid Interface Sci.* **1990**, 134, 475.
10. Fu, F.; Wang, Q. *J. Environ. Manage.* **2011**, 92, 407.
11. Savage, N.; Diallo, M. *J. Nanopart. Res.* **2005**, 7, 331.
12. Chouyyok, W.; Shin, Y.; Davidson, J.; Samuels, W. D.; LaFemina, N. H.; Rutledge, R. D.; Fryxell, G. E.; Sangvanich, T.; Yantasee, W. *Environ. Sci. Technol.* **2010**, 44, 6390.
13. Beatty, S. T.; Fischer, R. J.; Hagers, D. L.; Rosenberg, E. *Ind. Eng. Chem. Res.* **1999**, 38, 4402.
14. Beatty, S. T.; Fischer, R. J.; Rosenberg, E.; Pang, D. *Sep. Sci. Technol.* **1999**, 34, 2723.

15. Chen, Y.; Pan, B.; Li, H.; Zhang, W.; Lv, L.; Wu, J. *Environ. Sci. Technol.* **2010**, 44, 3508.
16. Gao, B.; An, F.; Liu, K. *Appl. Surf. Sci.* **2006**, 253, 1946.
17. Maketon, W. K.; Ogden, K.L. *IEEE Transactions on semiconductor manufacturing* **2008**, 21, 481.
18. Pang, Y.; Zeng, G.; Tang, L.; Zhang, Y.; Liu, Y.; Lei, X.; Li, Z.; Zhang, J.; Xie, G. *Desalination* **2011**, 281, 278.
19. Revathi, M.; Ahmed Basha, C.; Velan, M. *Desalin. Water Treat.* **2015**, 1.
20. Delacour, M. L.; Gailliez, E.; Bacquet, M.; Morcellet, M. *J. Appl. Polym. Sci.* **1999**, 73, 899.
21. Ghou, M.; Bacquet, M.; Morcellet, M. *Water Res.* **2003**, 37, 729.
22. Fischer, R. J.; Pang, D.; Beatty, S. T.; Rosenberg, E. *Sep. Sci. Technol.* **1999**, 34, 3125.
23. Duru, P. E.; Bektas, S.; Genç, Ö.; Patir, S.; Denizli, A. *J. Appl. Polym. Sci.* **2001**, 81, 197.
24. Navarro, R. R.; Sumi, K.; Fujii, N.; Matsumura, M. *Water Res.* **1996**, 30, 2488.
25. Chanda, M.; Pillay, S. A. *Indian J. Chem. Technol.* **2005**, 12, 156.
26. Deng, S.; Ting, Y.-P. *Water Res.* **2005**, 39, 2167.
27. Lindén, J. B.; Larsson, M.; Coad, B. R.; Skinner, W. M.; Nydén, M. *RSC Advances* **2014**, 4, 25063.
28. Lindén, J. B.; Larsson, M.; Kaur, S.; Skinner, W. M.; Miklavcic, S. J.; Nann, T.; Kempson, I. M.; Nydén, M. *RSC Advances* **2015**, 5, 51883.
29. Fitzpatrick, J. L.; Nadella, S.; Bucking, C.; Balshine, S.; Wood, C. M. *Comp. Biochem. Physiol., Part C: Toxicol. Pharmacol.* **2008**, 147, 441.
30. Schiff, K.; Brown, J.; Diehl, D.; Greenstein, D. *Mar. Pollut. Bull.* **2007**, 54, 322.
31. Abbott, G.; Brooks, R.; Rosenberg, E. *J. Appl. Polym. Sci.* **2015**, 132, 42271.
32. Ho, T. T. M.; Bremmell, K. E.; Krasowska, M.; Stringer, D. N.; Thierry, B.; Beattie, D. A. *Soft Matter* **2015**, 11, 2110.
33. Reviakine, I.; Johannsmann, D.; Richter, R. P. *Anal. Chem.* **2011**, 83, 8838.
34. Horcas, I.; Fernández, R.; Gómez-Rodríguez, J. M.; Colchero, J.; Gómez-Herrero, J.; Baro, A. M. *Rev. Sci. Instrum.* **2007**, 78, 013705.
35. Mészáros, R.; Thompson, L.; Bos, M.; de Groot, P. *Langmuir* **2002**, 18, 6164.
36. Mészáros, R.; Varga, I.; Gilányi, T. *Langmuir* **2004**, 20, 5026.
37. Tong, W.; Gao, C.; Möhwald, H. *Polym. Adv. Technol.* **2008**, 19, 817.
38. Sauerbrey, G. *Zeitschrift für Physik* **1959**, 155, 206.

39. Migneault, I.; Dartiguenave, C.; Bertrand, M. J.; Waldron, K. C. *BioTechniques* **2004**, 37, 790.
40. Biggs, T. W.; D'Anna, H. *Mar. Pollut. Bull.* **2012**, 64, 627.
41. Eriksen, R. S.; Mackey, D. J.; van Dam, R.; Nowak, B. *Mar. Chem.* **2001**, 74, 99.
42. Sekhar, C. K.; Chary, S. N.; Tirumala, K. C.; Aparna, V. *Acta Chim. Slov.* **2003**, 50, 409.
43. Sigg, L.; Xue, H. In *Chemistry of aquatic systems: local and global perspectives*; Bidoglio, G.; Stumm, W., Eds.; Springer Science & Business Media, **1994**; Chapter 7; pp 153-181.
44. Vraspir, J. M.; Butler, A. *Annual review of marine science* **2009**, 1, 43.

Figure Captions

Figure 1. QCM-D sensogram of the self-assembly of PEI (0.05, 0.1 and 0.2 wt% in 0.5 M NaCl in MQ-water, pH 9) onto silica-coated QCM sensors. Normalized frequency (top panel) and dissipation change (bottom panel) for the 5th overtone ($\nu = 5$), representative for quadruplicate experiments. The vertical dotted lines indicate the change of solution and the solutions are specified in-between the lines (MQ = MQ-water, AS = Artificial Seawater, NaCl = 0.5 M NaCl in MQ-water pH 9, PEI 1 = 0.05 wt% PEI in 0.5 M NaCl in MQ-water pH 9, HCl = 1 M HCl, PEI 2 = 0.1 wt% PEI in 0.5 M NaCl in MQ-water pH 9, PEI 3 = 0.2 wt% PEI in 0.5 M NaCl in MQ-water pH 9).

Figure 2. Zeta potential of branched polyethyleneimine (PEI) ($M_n \sim 60,000$ and $M_w \sim 750,000$, Sigma Aldrich, Australia) as a function of pH. The PEI concentration was 2 mg/mL in 1 mM KCl and pH was adjusted with 1 M HCl and 0.02 M KOH. Error bars indicate standard deviation of measurements ($n = 3$).

Figure 3. QCM-D sensogram of the cross-linking of self-assembled PEI on silica-coated QCM sensors. Normalized frequency (top panel) and dissipation change (bottom panel) for the 5th overtone ($\nu = 5$) of four simultaneously monitored sensors (S1 – S4). The vertical dotted lines indicate the change of solution and the solutions are specified in-between the lines (MQ = MQ-water and GA = 0.5 % glutaraldehyde in MQ-water). The reader is referred to the online version of the article for color figure.

Figure 4. The first row contains AFM height images ($1 \times 1 \mu\text{m}^2$) of (A) self-assembled PEI and (B) self-assembled and crosslinked PEI on silicon wafer. The middle row presents AFM 3D images of the coatings (scale bar same as top row). The bottom row shows relative height histograms for the AFM topographic images. The reader is referred to the online version of the article for color figure.

Figure 5. QCM-D sensogram of the acid stability of (A) self-assembled PEI and (B) crosslinked self-assembled PEI on silica-coated QCM sensors. Normalized frequency (top panel) and dissipation change (bottom panel) for the 5th overtone ($\nu = 5$), representative for quadruplicate experiments. The vertical dotted lines indicate the change of solution and the solutions are specified in-between the lines (MQ = MQ-water, NaCl = 0.5 M NaCl in MQ-water pH 9, PEI = 0.2 wt% PEI in 0.5 M NaCl in MQ-water pH 9, GA = 0.5 % GA in MQ-water, HCl = 1 M HCl, $\text{HNO}_3 = 1 \text{ M HNO}_3$).

Figure 6. A: Copper-to-nitrogen ratio and B: zinc-to-nitrogen ratio of crosslinked and non-crosslinked PEI coatings over time after immersion in artificial seawater (pH ~ 8.1) spiked with equimolar amounts of 12 seawater relevant metal ions (Al, Cd, Co, Cr, Cu, Fe, Mn, Mo, Ni, Pb, V and Zn. $[\text{Me}] \sim 3.15 \mu\text{M}$).

Except for copper and zinc, no other metals were detected in the coatings. Error bars indicate standard deviation of measurements ($n = 3$). Trend lines (dashed lines) were added as guidance for the eye.

Figure 7. Metal-to-nitrogen ratio of crosslinked and non-crosslinked PEI coatings after 128 min immersion in artificial seawater ($\text{pH} \sim 8.1$) spiked with equimolar amounts of 12 seawater relevant metal ions (Al, Cd, Co, Cr, Cu, Fe, Mn, Mo, Ni, Pb, V and Zn. $[\text{Me}] \sim 3.15 \mu\text{M}$). Except for copper and zinc, no other metals were detected in the coatings. Error bars indicate standard error of the mean ($n = 9$). * and ** indicate significant difference between means (* = $p < 0.02$ and ** = $p < 0.001$).

Figure 8. Metal-to-nitrogen ratio of crosslinked PEI coatings after immersion for 2 hours in artificial seawater ($\text{pH} \sim 8.1$) spiked with equimolar amounts of 12 seawater relevant metal ions (Al, Cd, Co, Cr, Cu, Fe, Mn, Mo, Ni, Pb, V and Zn. $[\text{Me}] \sim 3.15 \mu\text{M}$) for uptake (U) and MQ-water with pH adjusted to ~ 1 using hydrochloric acid (1 M) for release (R). Except for copper and zinc, no other metals were detected in the coatings. Error bars indicate standard error of the mean ($n = 3$). Numbers on x-axis indicate the number of cycles the samples have been through.

Figure 9. The first row contains AFM height images ($1 \times 1 \mu\text{m}^2$) of self-assembled and crosslinked PEI on silicon wafer (A) after preparation, (B) after the 10th uptake cycle and (C) after the 10th release cycle. The middle row presents AFM 3D images of the coatings (scale bar same as top row). The bottom row shows relative height histograms for the AFM topographic images. The reader is referred to the online version of the article for color figure.

Table Captions

Table 1. Frequency and dissipation changes for the 5th overtone upon adsorption of PEI from different concentrations, as determined by QCM-D. Standard deviation was determined from four experiments.

Table 2. Roughness analysis of PEI coatings on silicon wafers by AFM; SA = Self-assembled PEI, SA CL PEI = Self-assembled and crosslinked PEI, 10th uptake = Self-assembled and crosslinked PEI after 10th cycle of uptake, 10th release = Self-assembled and crosslinked PEI after 10th cycle of release. Error represents standard deviation where number of scans (n) was equal to or more than 3. Error for samples with number of scans less than 3 represent the difference of average from min/max.

Figure 1

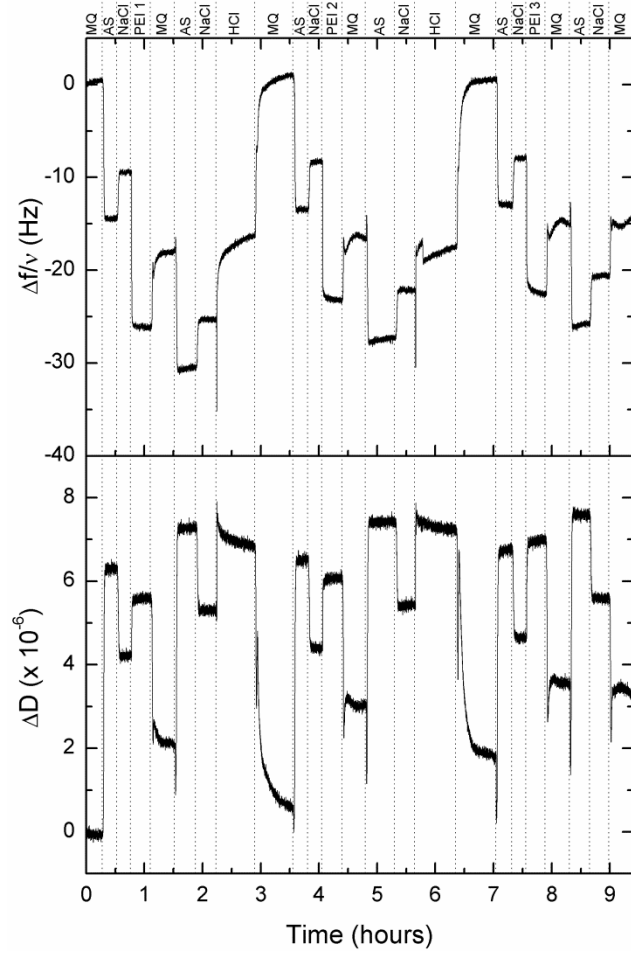


Figure 2

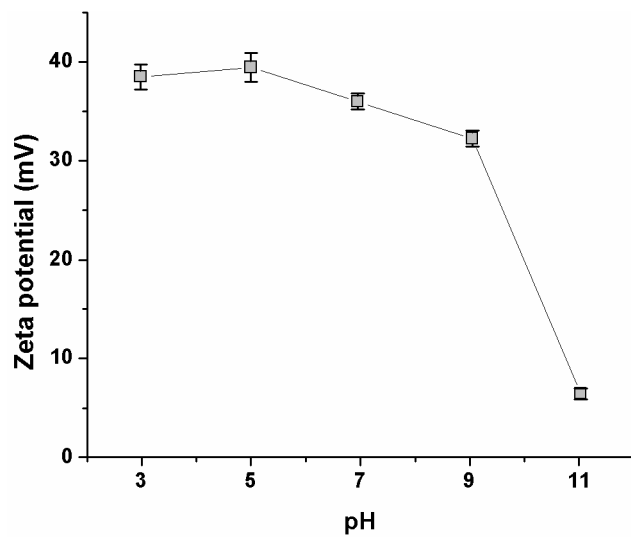


Figure 3

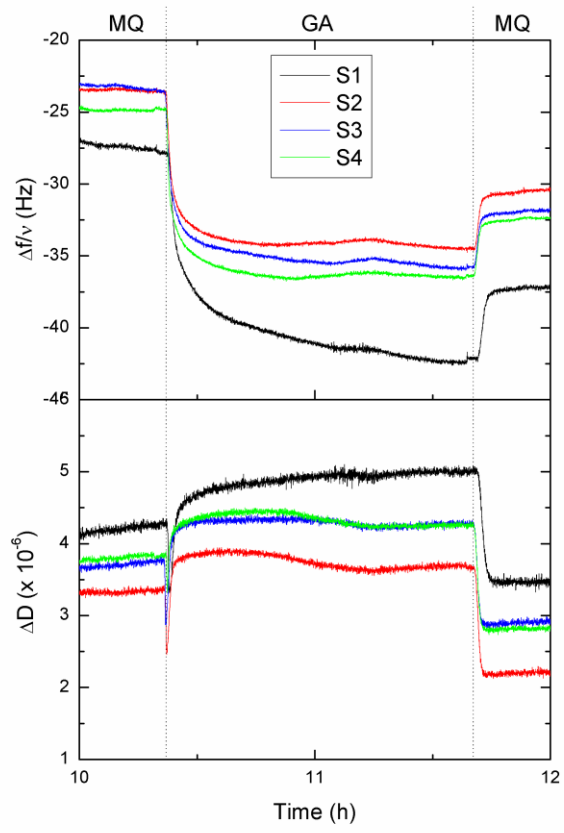


Figure 4

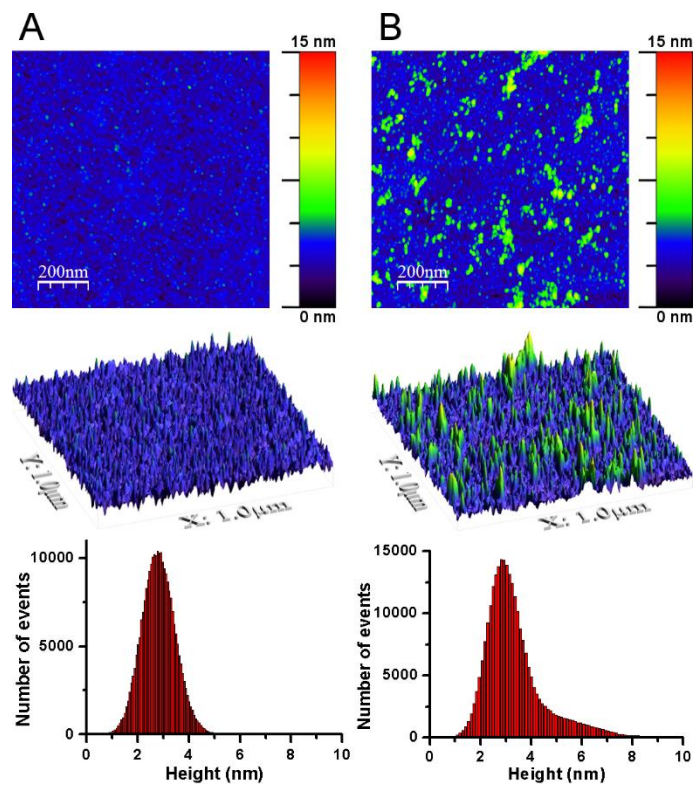


Figure 5

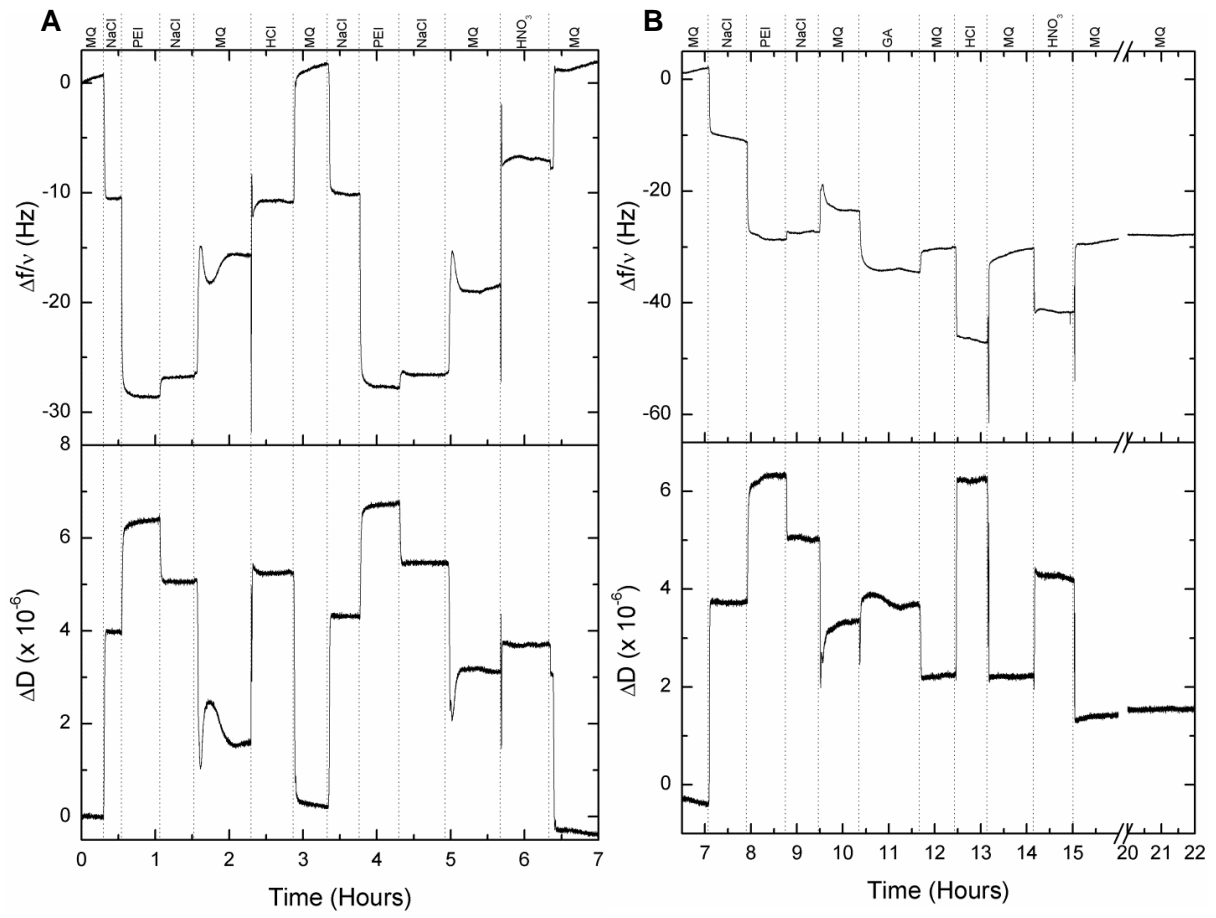


Figure 6

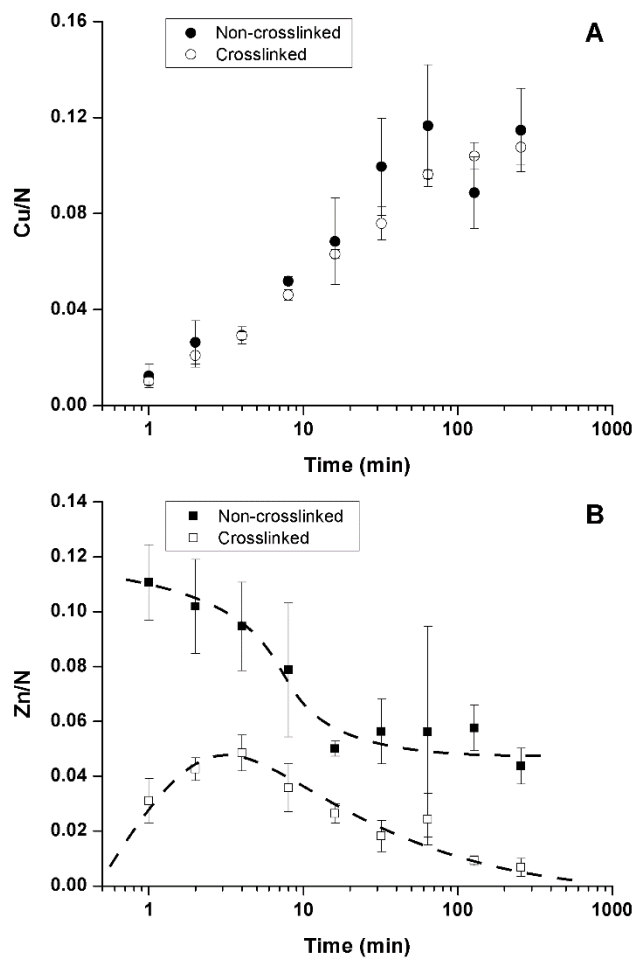


Figure 7

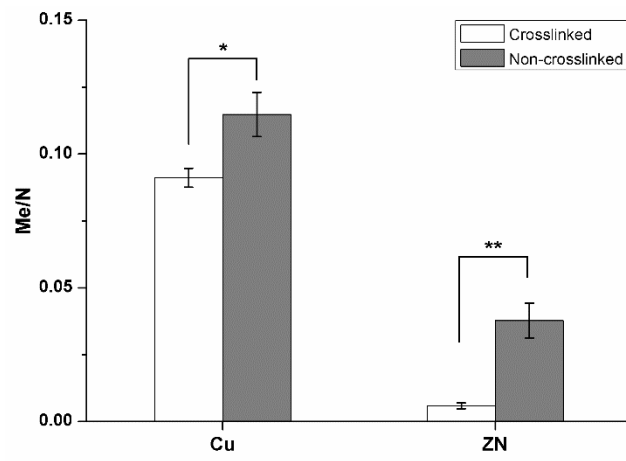


Figure 8

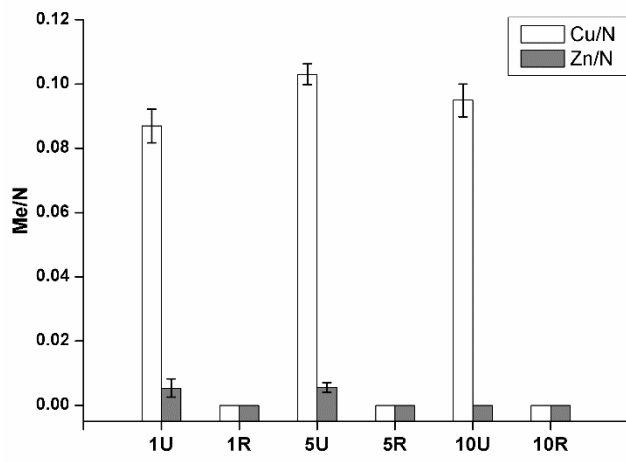
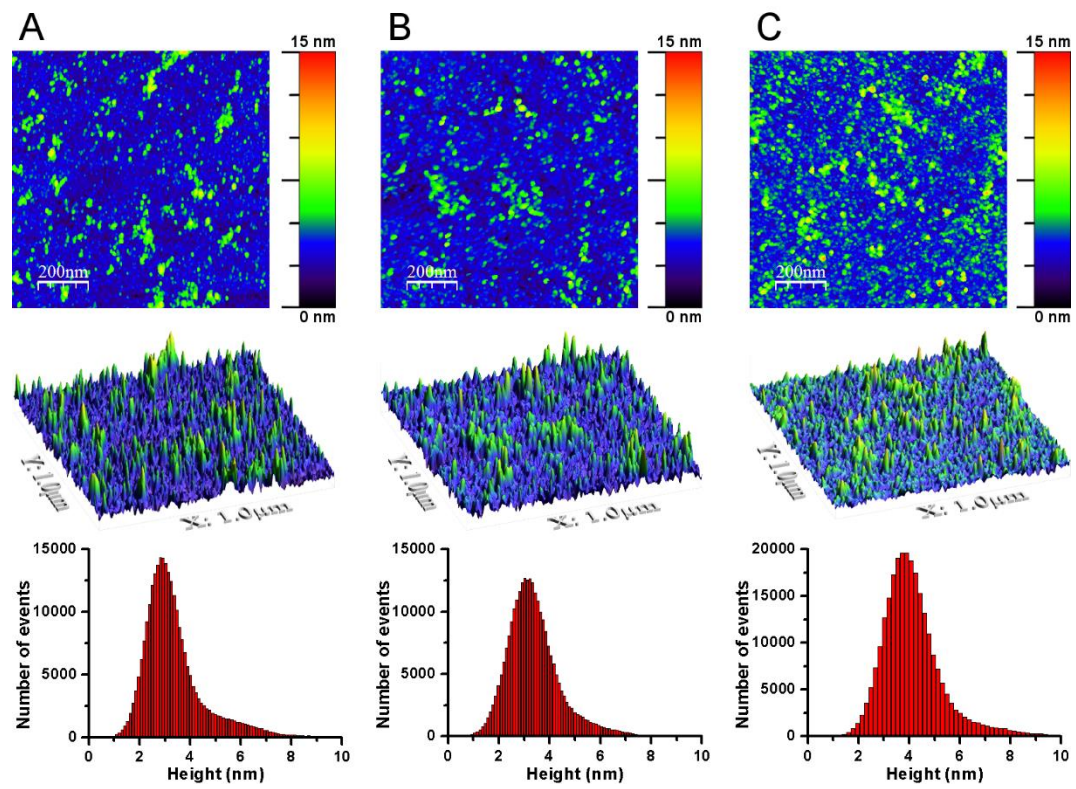


Figure 9



Tables

Table 1. Frequency and dissipation changes for the 5th overtone upon adsorption of PEI from different concentrations, as determined by QCM-D. Standard deviation was determined from four experiments.

PEI conc. (wt%)	$\Delta f/v$ (Hz)	ΔD ($\times 10^{-6}$)	Mass (ng/cm^2) ^a	Thickness (nm) ^b
0.05	- 17 \pm 1.3	1.6 \pm 0.7	300 \pm 23	2.9 \pm 0.2
0.10	- 15 \pm 4.5	2.0 \pm 1.3	260 \pm 80	2.6 \pm 0.8
0.20	- 15 \pm 3.6	2.0 \pm 1.1	270 \pm 63	2.7 \pm 0.6

^a Estimated using Sauerbrey relationship.³⁸

^b Calculated assuming a non-porous film with a density of 1 g/cm^3 .

Table 2. Roughness analysis of PEI coatings on silicon wafers by AFM; SA = Self-assembled PEI, SA CL PEI = Self-assembled and crosslinked PEI, 10th uptake = Self-assembled and crosslinked PEI after 10th cycle of uptake, 10th release = Self-assembled and crosslinked PEI after 10th cycle of release. Error represents standard deviation where number of scans (n) was equal to or more than 3. Error for samples with number of scans less than 3 represent the difference of average from min/max.

Sample	RMS (Rq) Roughness (nm)	Average (Ra) Roughness (nm)	Skewness (Rsk)	Average height (nm)	Number of scans (n)
SA PEI	0.69 ± 0.05	0.54 ± 0.04	0.2 ± 0.1	2.9 ± 0.3	7
SA CL PEI	1.25 ± 0.09	0.91 ± 0.07	1.4 ± 0.2	3.6 ± 0.3	4
10 th uptake	1.06 ± 0.03	0.78 ± 0.02	1.2 ± 0.03	3.3 ± 0.1	2
10 th release	1.22 ± 0.02	0.88 ± 0.02	1.5 ± 0.08	3.9 ± 0.3	2

SUPPORTING INFORMATION

Glutaraldehyde-crosslinking for improved copper absorption selectivity and chemical stability of polyethyleneimine coatings

Johan B. Lindén^a, Mikael Larsson^{a, b}, Simarpreet Kaur^a, Ataollah Nosrati^c and Magnus Nydén^{a, b}

^aFuture Industries Institute, University of South Australia, Mawson Lakes, SA, 5095, Australia.

^bSchool of energy and resources, University College London, 220 Victoria Square, Adelaide, SA, 5000, Australia.

^cSchool of Engineering, Edith Cowan University, 270 Joondalup Drive, Joondalup WA, 6027, Australia.

Correspondence to: M. Larsson (E-mail: larsson.mikael@gmail.com)

AFM height images and roughness analysis of PEI coatings on silicon wafer after self-assembly, crosslinking and cycles of copper uptake and release.

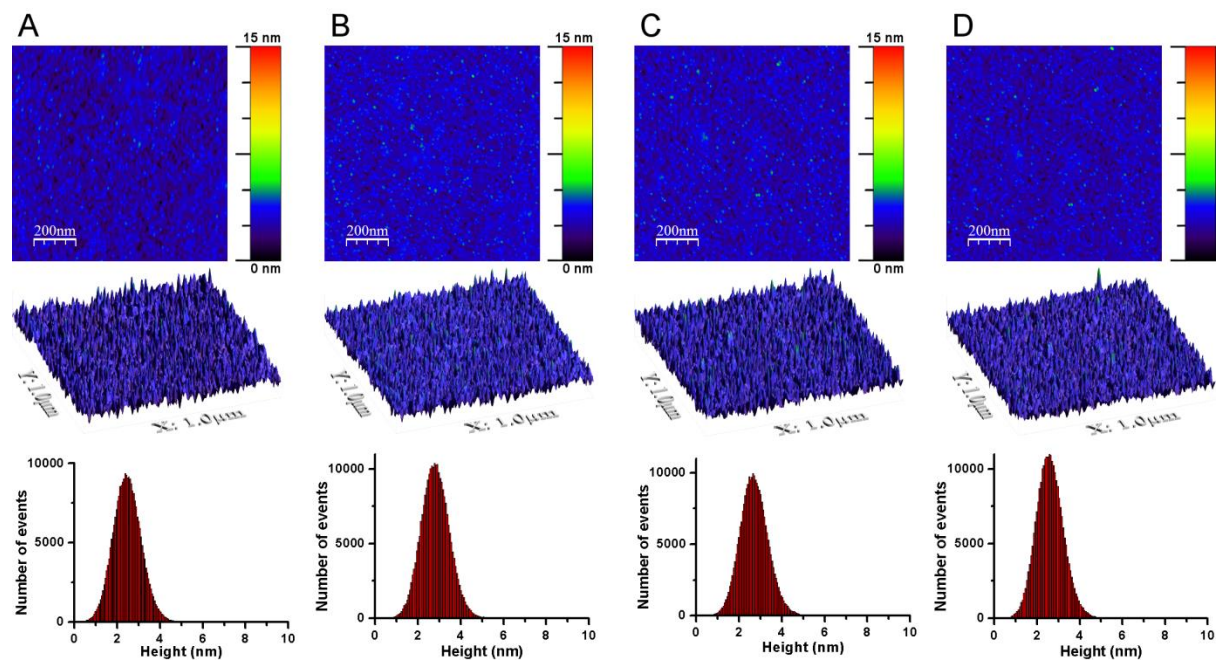


Figure S1. The first row contains AFM height images ($1 \times 1 \mu\text{m}^2$) of self-assembled PEI on silicon wafer at four different locations on the sample. The middle row presents AFM 3D images of the coatings (scale bar same as top row). The bottom row shows relative height histograms for AFM topographic images.

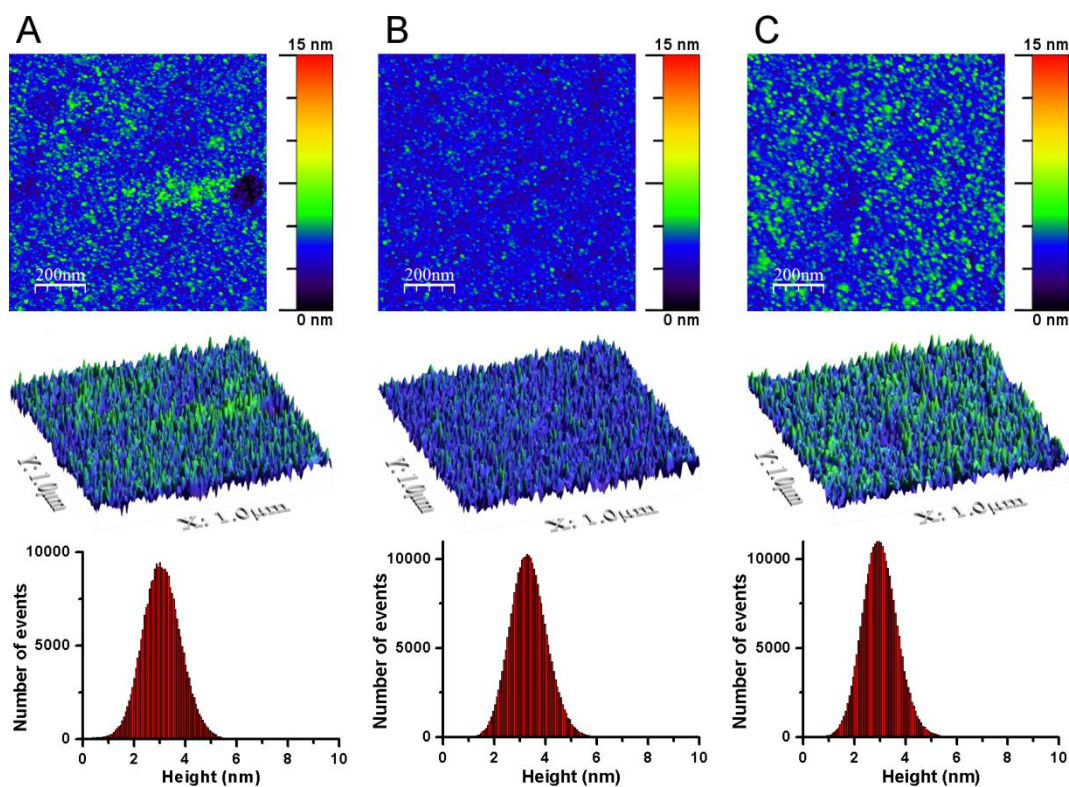


Figure S2. The first row contains AFM height images (1 × 1 μm²) of self-assembled PEI on silicon wafer at three different locations on the sample. The middle row presents AFM 3D images of the coatings (scale bar same as top row). The bottom row shows relative height histograms for AFM topographic images.

Note that for Figure S5 A and B the data ranges were limited to exclude events from coating defects with very low prevalence, that otherwise caused a shift in the height of the surface plane that made comparison more difficult. In other words, the coatings were close to identical with regards to surface roughness, any differences were from rare and non-representative defects.

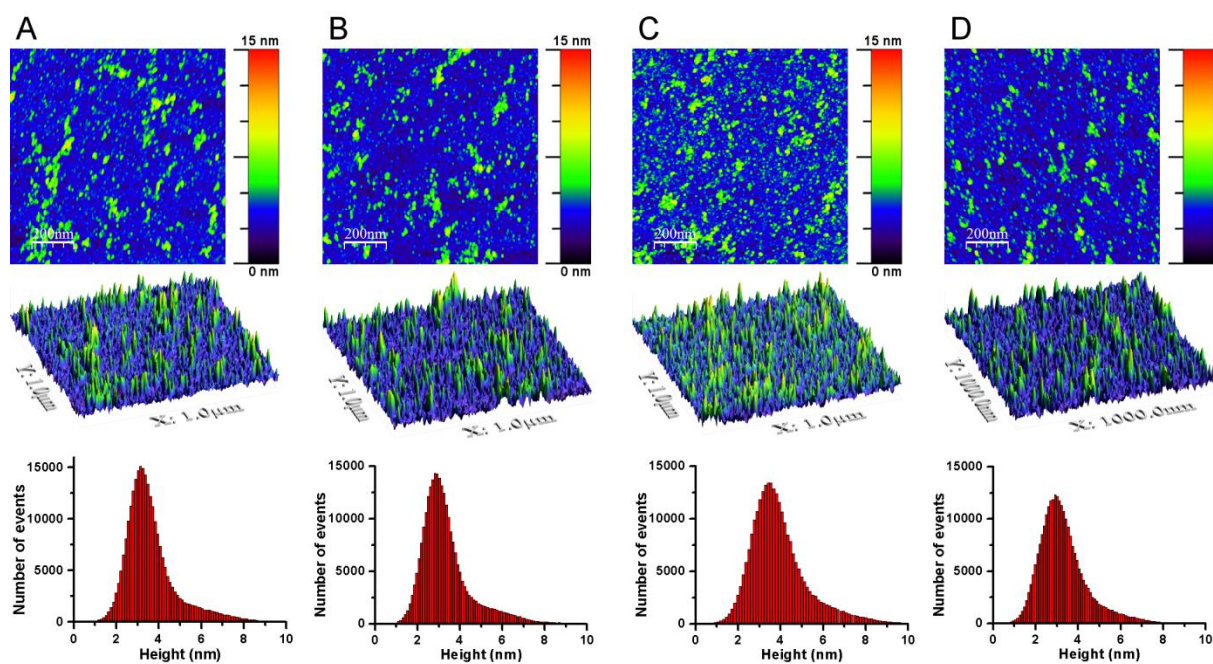


Figure S3. The first row contains AFM height images ($1 \times 1 \mu\text{m}^2$) of self-assembled and crosslinked PEI on silicon wafer. (A) and (B) represents scans at different locations on one sample and (C) and (D) represents scans at different locations on a different sample. The middle row presents AFM 3D images of the coatings (scale bar same as top row). The bottom row shows relative height histograms for AFM topographic images.

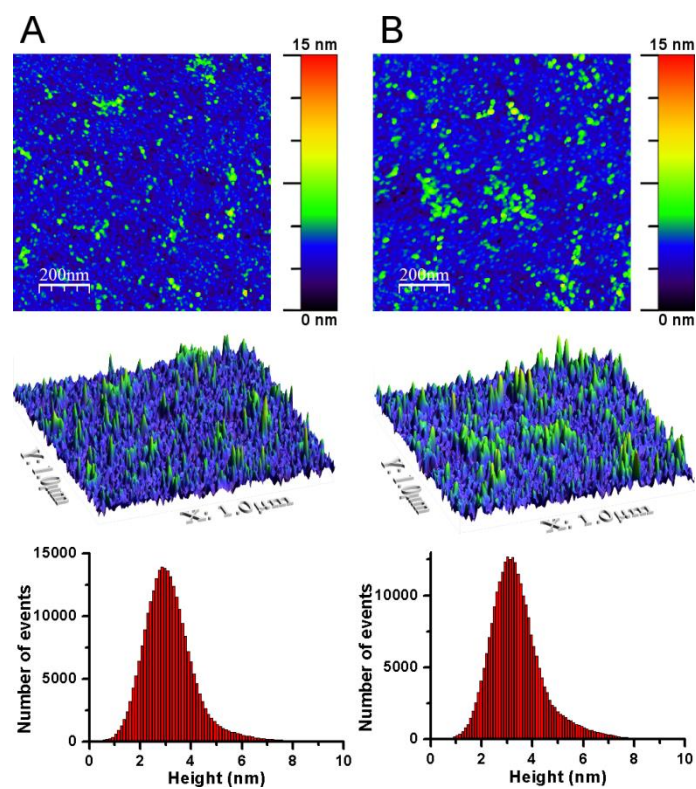


Figure S4. The first row contains AFM height images ($1 \times 1 \mu\text{m}^2$) of scans at two different locations on self-assembled and crosslinked PEI on silicon wafer after the 10th uptake cycle. The middle row presents AFM 3D images of the coatings (scale bar same as top row). The bottom row shows relative height histograms for AFM topographic images.

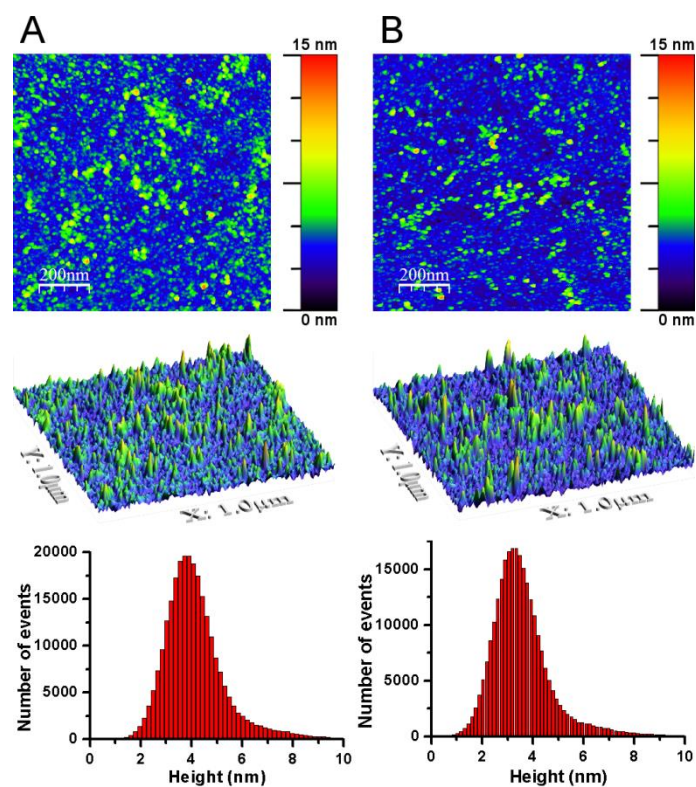


Figure S5. The first row contains AFM height images ($1 \times 1 \mu\text{m}^2$) of scans at two different locations on self-assembled and crosslinked PEI on silicon wafer after the 10th release cycle. The middle row presents AFM 3D images of the coatings (scale bar same as top row). The bottom row shows relative height histograms for AFM topographic images.

QCM-D sensogram of the stability of non-crosslinked and crosslinked self-assembled of PEI on silica-coated QCM sensors in artificial seawater.

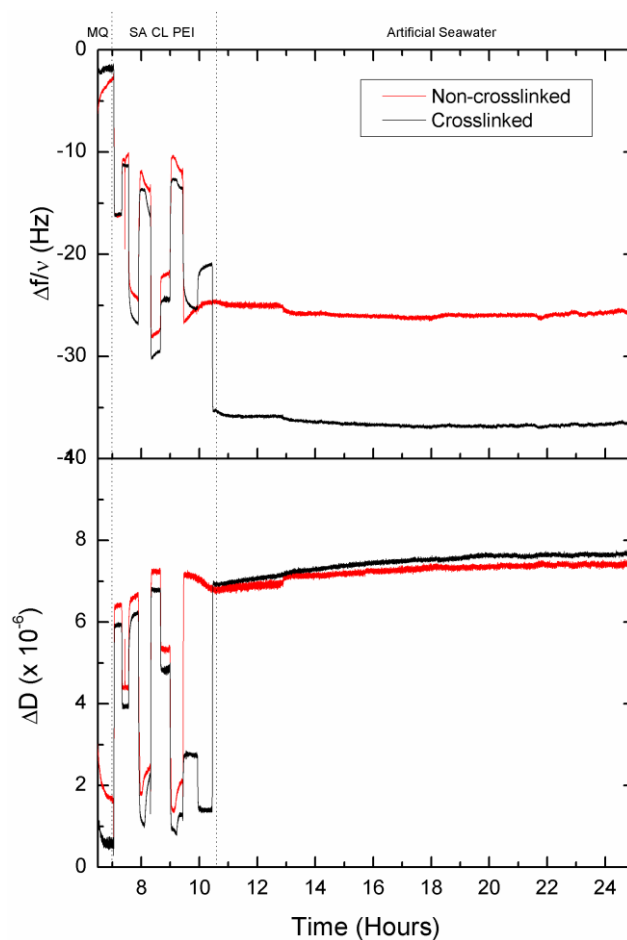


Figure S6. QCM-D sensogram of the stability of non-crosslinked and crosslinked self-assembled of PEI on silica-coated QCM sensors in artificial seawater. Normalized frequency (top panel) and dissipation change (bottom panel) for the 5th overtone ($\nu = 5$). The vertical dotted lines indicate the change of solution and the solutions are specified in-between the lines (MQ = MQ-water and SA CL PEI = self-assembly and crosslinking of PEI).